Alexandria Engineering Journal (2015) 54, 1273–1284

Alexandria University

Alexandria Engineering Journal

www.elsevier.com/locate/aej
www.sciencedirect.com

ORIGINAL ARTICLE

Removal of fluoride by aluminum impregnated coconut fiber from synthetic fluoride solution and natural water

Naba Kumar Mondal *, **Ria Bhaumik**, **Jayanta Kumar Datta**

Department of Environmental Science, The University of Burdwan, Burdwan, India

Received 16 June 2015; revised 30 July 2015; accepted 20 August 2015
Available online 14 September 2015

KEYWORDS

Coconut fiber;
Fluoride;
Adsorption;
Desorption;
Co-ions;
Thermodynamic parameters

Abstract Aluminum impregnated coconut fiber ash (AICFA) was used for removal of fluoride from synthetic fluoride solution. The AICFA showed high specific area and strong affinity toward fluoride. Synthesized AICFA was characterized by pH_{ZPC}, FTIR, SEM and XRD studies. Adsorption kinetics indicated that the adsorption equilibrium was reached within 60 min and the adsorption process followed the pseudo-second-order kinetic model better. The Langmuir isotherm model could fit the experimental data well. Thermodynamic parameters such as Gibbs free energy (ΔG°), enthalpy (ΔH°) and entropy (ΔS°) change of sorption were also evaluated which indicated that the adsorption process was spontaneous, feasible and exothermic in nature. Furthermore, the coexisting anions had significant effect on fluoride adsorption. Moreover, desorption study with AICFA showed that nearly 98% of fluoride could be leached out at pH 12. Further, the reusable properties of the material supported the possibility of its use commercially.

1. Introduction

Toxicity of hazardous ions, such as fluoride, is of interest for public health [1,2]. It is the strongest electronegative elements and in gaseous form is a very powerful oxidizing agent [3]. The natural abundance of fluoride ranges from 0.065% to 0.09% by weight in the earth's crust and it exists naturally as fluoride ions (F^-) which is extremely reactive [3]. The main source of fluoride for humans is drinking water contaminated by geological sources [4,5]. Fluoride at micro-molar level is considered as an effective anabolic agent because it promotes cell proliferations, whereas in millimolar concentration, it can bind to the functional amino acid groups located around the active center of an enzyme to cause an inhibitory effect which leads to decrease enzyme activity [6,7]. According to World Health organization (WHO), the acceptable limit of fluoride in drinking water is 1.5 mg L^{-1} [8]. In some areas of India a typical fluoride concentration in underground water is found to be in the range of 1.5–6.5 mg L^{-1} [9].

A number of drinking water defluoridation techniques have been developed. Among them reverse osmosis (RO), is one of the well-known techniques applied for removal of fluoride [10]. However, RO has serious drawback for its high operational and maintenance costs. Application of solar distillation for

* Corresponding author. Cell: +91 9434545694; fax: +91 (342) 2634200.
E-mail address: nkmenvbu@gmail.com (N.K. Mondal).
Peer review under responsibility of Faculty of Engineering, Alexandria University.

http://dx.doi.org/10.1016/j.aej.2015.08.006

defluoridation demonstrated approximately 97% fluoride removal [11]. But the method does not produce large volume of potable water, which is its serious drawback. On the other hand, nanofiltration shows remarkable suitability for defluoridation of water. However, the use of inorganic component such as $CaCO_3$ as filter and membrane produces a smell in the water. In addition, this method requires a huge maintenance cost [12]. Application of precipitation and coagulation method for defluoridation of water has also been investigated [13,14]. However, the shortcomings of most of these methods are high operational and maintenance costs, secondary pollution (generation of toxic sludge, etc.) and complicated procedure involved in the treatment [15].

In comparison with the abovementioned techniques for defluoridation of water, adsorption is a simple, low cost and easily applicable method [16,17]. Literature has reported various adsorbents for defluoridation such as egg cell dust, sugarcane rice husk ash, tea ash, leaf biomass, algal biomass, sugarcane baggies charcoal, bio-char, etc [18–20,16,21,22].

The interest in fluoride removal by biomass based adsorbents is growing due to their low cost and availability. It is well reported that functional groups such as hydroxyl, carbonyl, amine, amide, carboxyl, sulfhydryl, imidazole, phosphonate, and phosphodiester present on the biosorbent surface contributed to biosorption [23–25]. Nowadays, it is a great challenge in the area of public health to remove fluoride from drinking water by using low-cost adsorbents at local levels, especially in fluoride affected areas. Moreover, field sample was collected from fluoride affected area of Birbhum district, West Bengal, where plenty of coconut trees are available. With this in perspective, present work was undertaken to explore the potentiality of aluminum impregnated coconut fiber ash for removal of fluoride from synthetic fluoride solution.

2. Materials and methods

2.1. Collection of adsorbents

The coconut fiber was collected from fruit shops of local market (24°35′0″N latitude and 87°5′25″E longitude). After collection it was cut into small pieces and dried in sunlight. After drying it was burned in muffle furnace at 423 K for one and half hours. The ash was washed with distilled water, dried in sunlight and then dried in oven at 353 K for overnight. It was sieved through mesh size of 150 mm and kept in plastic air tied container for further use. This material considered as coconut fiber ash (CFA). All chemical reagents were of analytical grade. Deionized water was used throughout the experiments.

2.2. Preparation of aluminum coated CFA

2.2.1. Method of coating of aluminum hydroxide on CFA

According to Ganvir and Das [26] aluminum impregnation has been done by using stirred tank reactor with stirring, vacuum/pressure filter and oven/drier (Fig. 1). Initially, 100 g CFA was taken in stirred reactor tank and 500 mL of 0.6 M aluminum sulfate solution was added and stirred the mixture. The reactor was stirred at 180–200 rpm with 1.0 M sodium hydroxide solution. In this condition, sodium hydroxide reacts with aluminum sulfate to produce aluminum hydroxide which gets deposited on CFA. In this process, the addition of sodium hydroxide is very vital and it was controlled by proper checking of pH of the mixture. Once the pH of the reaction media reaches the desired value of 5–7, sodium hydroxide addition was stopped. Finally the resulting adsorbent contains the mixture of sodium sulfate and aluminum hydroxide coated CFA. Thereafter, the whole slurry was filtered and subsequently dried at 400 K to get the desired adsorbent. However, for further use the CFA was thoroughly washed with double distilled water in order to complete removal of sodium sulfate and dried in oven at 370 K.

2.2.2. Adsorbent characterization

The scanning electron microscopy (SEM) images of the adsorbent sample are helpful to understand its surface structure. In this study images were recorded by using SEM analyzer (HITACHI, S-530, Scanning Electron Microscope and ELKO Engineering) at an accelerating voltage of 20.0 kV. Automated Mercury Porosimeters (Quantachrome, model Pore Master 60 GT) were used to determine the pore size distribution since this method is suitable for determining larger pores such as mesopores or micropores. The FTIR study was done to record the potential functional groups involved in the adsorption process by using FTIR (BRUKER, Tensor 27). The crystalline structure of the adsorbent was characterized using Ni-filtered Cu Kα radiation from a highly stabilized and automated Philips X-ray generator (XRD, PW 1830) operated at 35 kV and 25 mA at a scanning speed of 2° min^{-1} from 10° to 70°. The XRD data were matched with standard JCPDS data.

2.3. Adsorption experiment

An artificial fluoride solution was prepared by dissolving 2.21 g sodium fluoride solid granules in 1 L of deionized water and subsequently diluted to the required concentrations for the adsorption experiments. The adjustment for pH was done using HCl or NaOH. All the experiments were carried out in 250 mL conical flask, with 100 mL F^- solutions at different experimental temperature. These flasks, along with test solution and adsorbent, were shaken by the magnetic starrier, to study various parameter. The percentage of fluoride removal (% F) and the amount of F adsorbed per unit weight of adsorbent at time t (q_t, mg g^{-1}) and at equilibrium (q_e, mg g^{-1}) were calculated using the following equation, respectively:

$$\%F = \frac{C_0 - C_e}{C_0} \times 100 \quad (1)$$

$$q_t = \frac{(C_0 - C_t)v}{m} \quad (2)$$

$$q_e = \frac{(C_0 - C_e)v}{m} \quad (3)$$

where v (L) is the volume of fluoride solution, and C_0 (mg L^{-1}) is the initial concentration of F. C_t (mg L^{-1}) is the concentration of F at a given time t, C_e (mg L^{-1}) is the concentration of F at equilibrium and m(g) is the dry weight of the adsorbents. The relative parameters for the isotherm and kinetic equations were obtained using χ^2 relationship between the calculated and

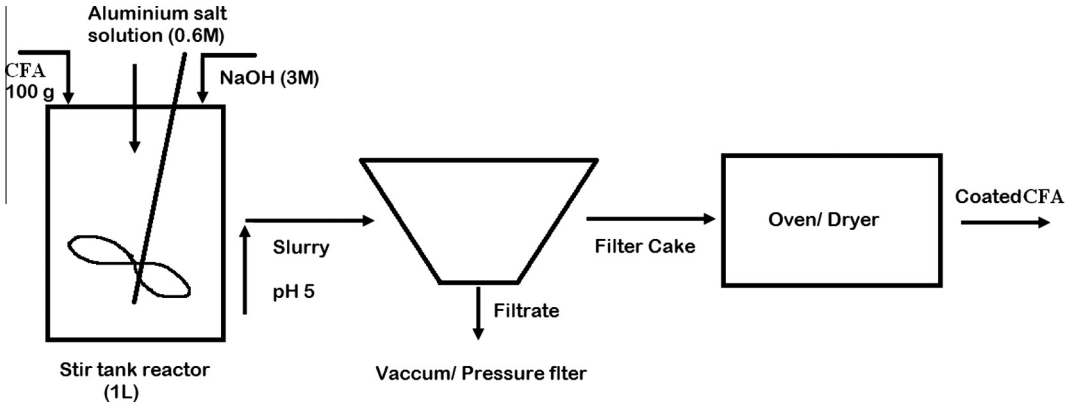

Figure 1 Process flow sheet of aluminum hydroxide coating on coconut fiber ash (CFA). (Figure adopted and modified from Ganvir and Das [26]).

experimental data employing non-linear analysis. The calculated expression for chi-square, χ^2 may be written as follows:

$$\chi^2 = \sum \frac{(q_{e,\exp} - q_{e,\mathrm{cal}})2}{q_{e,\mathrm{cal}}} \tag{4}$$

where $q_{e,\exp}$ is experimental equilibrium capacity data and $q_{e,\mathrm{cal}}$ is the equilibrium capacity from a model. If data from the model are similar to experimental data, χ^2 will be small and if they differ, χ^2 will be large.

2.4. Adsorption isotherm analysis

The experimental data obtained at equilibrium isotherm of fluoride adsorption by AICFA were fitted to the frequently used models, Langmuir and Freundlich absorption isotherm [27].

$$\frac{1}{q_e} = \frac{1}{q_0 \beta C_e} + \frac{1}{q_0} \tag{5}$$

$$\log q_e = \log K_f + \frac{1}{n} \log C_e \tag{6}$$

where q_e is the amount of solute adsorbed per unit weight of material (mg/g), q_0 is the maximum adsorption capacity (mg/g), β is the Langmuir constant, K_f is the minimum sorption capacity (mg/g), n is the adsorption intensity of the Freundlich isotherm, and C_e is the equilibrium concentration of fluoride (mg/L). The isotherm parameters are shown in Table 1. The applicability of the isotherm equation was compared by evaluating the correlation co-efficient (R^2). It is revealed from the results that Langmuir isotherm model is the fittest fluoride adsorption process on AICFA. The Freundlich isotherm reveals adsorption capacity of 3.14 mg/g for AICFA, which is much higher than for granular red mud, at 0.85 mg/g [28].

D–R isotherm is more general than the Langmuir because it does not assume a homogeneous surface or constant sorption potential. D–R model is expressed by Eqs. (15) and (16), where β is the activity coefficient related to mean sorption energy (mol^2 kJ^{-2}); ε is the Polanyi potential, R is the ideal gas constant, T is the absolute temperature and E (kJ mol^{-1}) is defined as the free energy change required to transfer 1 mol of ions from solution to the solid surfaces, which equals to the following equation:

$$\ln q_e = \ln q_m - \beta \varepsilon^2 \tag{7}$$

$$\varepsilon = RT \ln \left(1 + \frac{1}{C_e}\right) \tag{8}$$

$$E = \frac{1}{\sqrt{2\beta}} \tag{9}$$

The magnitude of E is useful for estimating the type of sorption reaction. The calculated free energy values suggested the participation of physical forces during sorption [29,30].

2.5. Adsorption kinetic studies

2.5.1. Kinetic rate parameters

$$\log(q_e - q_t) = \log q_e - \frac{k_1 t}{2.303} \tag{10}$$

$$\frac{t}{q_t} = \frac{1}{k_2 t^2} + \frac{t}{q_e} \tag{11}$$

$$q_t = K_d t^{1/2} \tag{12}$$

$$D_f = 0.23 \times r_0 \delta \frac{\overline{C}}{C} t^{1/2} \tag{13}$$

where q_t and q_e are the amount of the adsorbed fluoride (mg/g) at time t and at equilibrium time, respectively and K_1 and K_2 are first order and second order rate constants for adsorption. K_d is the intraparticle diffusion rate constant (mg g^{-1} min$^{-0.5}$). The results are shown in Table 2. The correlation coefficient value for the pseudo-second order adsorption model (R^2 = 0.9993) is much higher than that obtained for the pseudo first order kinetics (R^2 = 0.8049). On the other hand D_f is the diffusion coefficient expressed in cm^2/s, r_0 is the radius of the sorbent expressed in cm, $t^{1/2}$ is the half-life period in sec, δ is the film thickness expressed in cm and $\frac{\overline{C}}{C}$ is equilibrium loading of the sorbent.

2.6. Distribution coefficient

A distribution coefficient, K_D, reflects the binding ability of the surface for an element and is dependent on pH of the solution and type of surface of the adsorbent. The distribution coefficient values for fluoride adsorbed on CFD at pH 6.0 were calculated [31] using the following equation:

Table 1 Isotherms constant for adsorption of fluoride onto AICFA.

Temperature (K)	Langmuir				Freundlich				D–R			
	q_m (mg g^{-1})	K_L (L mg^{-1})	R^2	χ^2	q_m (mg g^{-1})	K_F	n	R^2	χ^2	q_m (mg g^{-1})	β (mol^2 kJ^{-2})	E (kJ mol)	R^2	χ^2
313	1.128	0.183	0.942	0.275	3.192	0.301	0.797	0.440	64.302	3.412	0.581	0.927	0.893	0.314
333	5.60	12.273	0.975	0.503	4.95	5.984	1.235	0.155	8.191	5.621	0.593	0.918	0.867	0.621
353	5.827	12.636	0.954	0.714	6.104	0.004	0.306	0.914	61.66	5.718	0.611	0.946	0.899	0.411
373	5.619	11.000	0.972	1.182	6.004	0.036	0.767	0.068	44.27	5.331	0.732	0.826	0.831	0.451

$$K_D = \frac{C_s}{C_w}(\mathrm{m^3/kg}) \tag{14}$$

where C_s is the concentration of fluoride on the solid particles (mg/kg) and C_w is the equilibrium concentration in solution (mg/m^3).

3. Results and discussion

3.1. Characterization of AICFA

The surface morphology of the AICFA examined by SEM (Figs. 2a and 2b) clearly revealing a smooth layer surface structure shows high adsorption capacity. The SEM structure of AICFA before and after adsorption of fluoride showed little variation in surface structure. This change of surface chemistry is due to the introduction of foreign ions (Al) [32]. Figs. 2a and 2b compare the surface features of adsorbents before and after fluoride adsorption at a magnification of 2000×. On the other hand, X-ray powder diffraction was studied to analyze the existence of aluminum in AICFA (Fig. 2c). From Fig. 2c, the presence of aluminum in AICFA (2θ, 39.65) is clear. XRD analysis directly provides evidence that aluminum was impregnated in coconut fiber. The surface areas of unimpregnated coconut fiber and AICFA were recorded as 20.4 and 26.3 m^2/g, respectively. Results clearly revealed that AICFA showed little higher surface area than unimpregnated coconut fiber. This is perhaps due to the uniform coating of alum on the surface of the coconut fiber, and hence the increase in the pore volume [33]. However, exactly opposite result can be expected. This is because on impregnation, surface area of impregnated adsorbent usually decreases due to the diffusion of impregnated particles into the pores of the adsorbent [34]. The FTIR spectra of AICFA before and after fluoride adsorption are shown in Figs. 3a and 3b. The FTIR spectral analysis of AICFA shows distinct peaks at 3436, 2363 and 2345 cm^{-1}. The broad and strong bend at 3436 cm^{-1} indicates the presence of —OH stretching. The —CH_2 stretching vibration could be ascribed to the band that appeared at 2363 cm^{-1}. The strong peak at 2345 cm^{-1} indicates the presence of —C≡C group while adsorption at 1404 cm^{-1} is due to —N—H vibration. Thus, FTIR spectral

Table 2 Kinetics constant for adsorption of fluoride onto AICFA.

Kinetic model	Parameters	Temperature (K)			
		313	333	357	373
Pseudo-first order	$q_{e,\exp}$ (mg/g)	3.13	2.21	1.67	0.612
	$K_1 \times 10^2$ (min^{-1})	1.039	0.409	0.768	0.456
	R^2	0.809	0.818	0.847	0.787
	χ^2	0.431	0.633	0.539	0.446
Pseudo-second order	$q_{e,\exp}$ (mg/g)	1.13	2.76	0.931	0.411
	K_2 (g/mg min)	0.416	3.889	1.790	3.545
	R^2	0.999	0.983	0.980	0.915
	χ^2	0.313	0.631	0.611	0.431
Intra-particle diffusion	$k_{id} \times$ (mg/g min$^{0.5}$)	88.703	5.627	4.853	3.421
	R^2	0.688	0.948	0.928	0.929
	χ^2	0.331	0.635	0.411	0.661

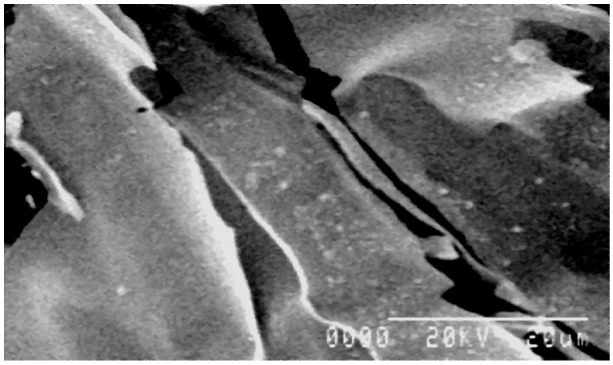

Figure 2a Aluminum impregnated coconut fiber ash (before fluoride stress) (magnification 500×).

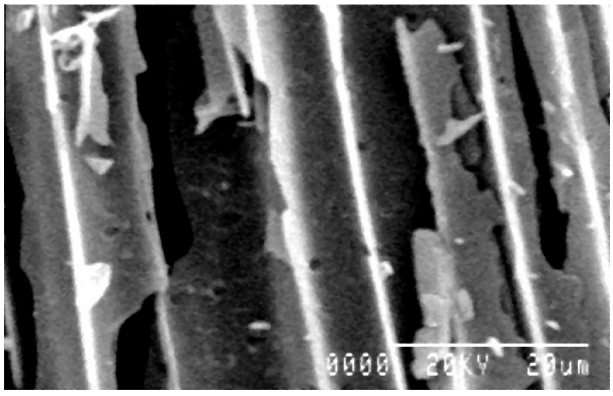

Figure 2b Aluminum impregnated coconut fiber ash (after fluoride stress) (magnification 500×).

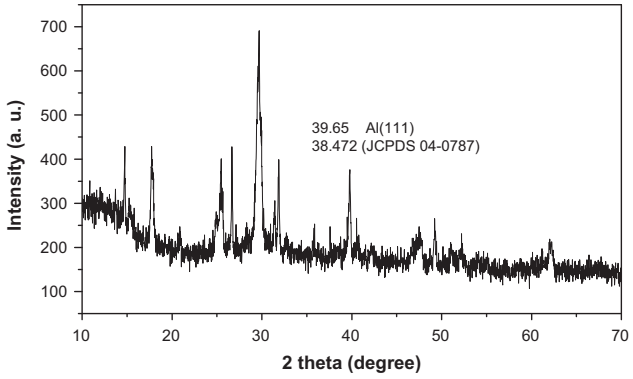

Figure 2c XRD of coconut fiber under aluminum loaded condition.

analysis demonstrates that the functional groups such as alcoholic groups and unsaturation dominate the surface of AICFA. After fluoride adsorption the intensity of hydroxyl carbonate and halide bowls of the adsorbent is reduced compared to that of the adsorbent before adsorption of fluoride. Strong adsorption band of 3436 cm^{-1} (—OH stretching) was shifted to 3443 cm^{-1} after fluoride adsorption. These results suggest that fluoride interacts with the —OH and —NH groups present on AICFA surface. Similar shifting of adsorption band

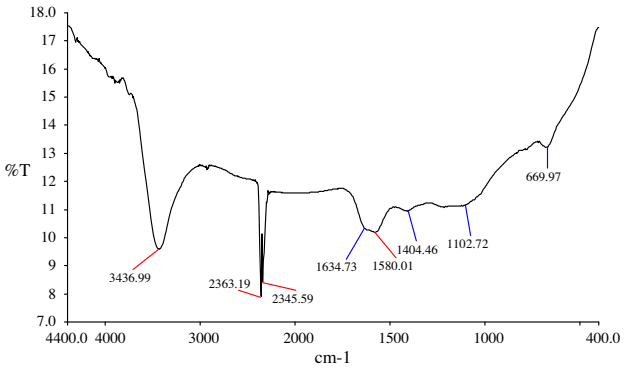

Figure 3a AICFA before adsorption of fluoride.

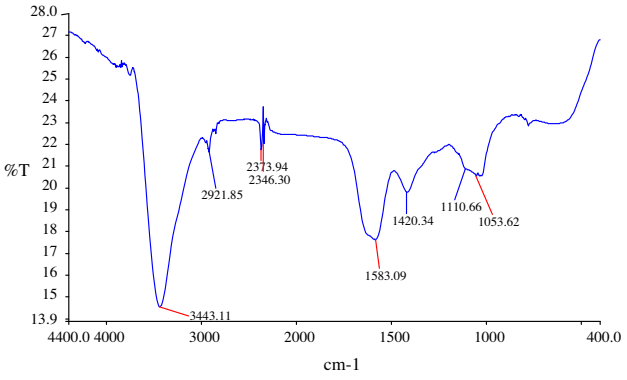

Figure 3b AICFA after adsorption of fluoride.

was reported earlier by Mondal et al. [18]. Moreover, transmission bands at 1420 and 1583 cm^{-1} are more dominant in case of fluoride sorbed on AICFA. This observation suggests possible interaction between fluoride and AICFA. A similar observation was reported by Vences-Alvarez et al. [35] in their work on fluoride sorption by hybrid adsorbent-lanthanum carbon.

3.2. Effect of pH

Fig. 4 indicates that maximum fluoride adsorption occurs at pH 5 which is below the pH_{zpc} of AICFA. Fluoride removal was not satisfactory at pH below 5. This can be attributed to the distribution of F^- and HF which are controlled by pH of the aqueous solution [36]. However calculation (Eq. (15)) showed that fluoride ion is the dominated species when pH of the solution exceeds the pK_a (3.16) value of HF [37].

$$P_{ions} = \frac{1}{[1 + 10^{(pK_a - pH)}]} \tag{15}$$

Results also revealed that F^- removal significantly reduced when pH of the solution increased to 8 or higher (Fig. 4). This might be attributed to the pH_{zpc} of AICFA (Fig. 5). The surface charge of the pH_{zpc} is usually assessed by the zero point charge (pH_{zpc} = 7.2), and at pH < pH_{zpc}, the surface charge is positive, at pH = $pH_{zpc,}$ the surface charge is neutral, and at pH > $pH_{zpc,}$ the surface charge is negative [38]. At a pH, above pH_{zpc} more of the surface sites are negatively charged and subsequently electrostatic repulsion occurs between

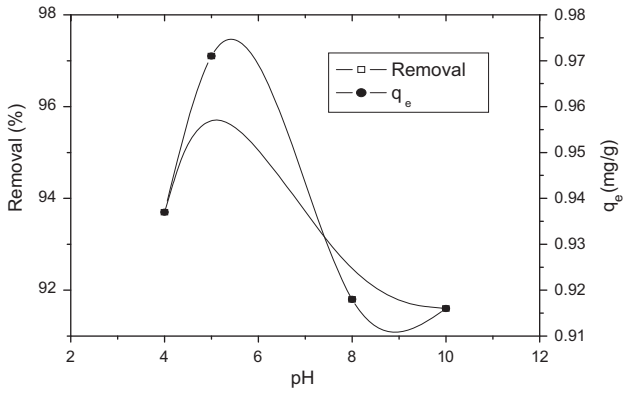

Figure 4 Effect of pH on removal of fluoride from water (initial conc. = 1 mg/L, adsorbent dosage = 0.05 g/L, contact time = 1 h, temperature = 313 K).

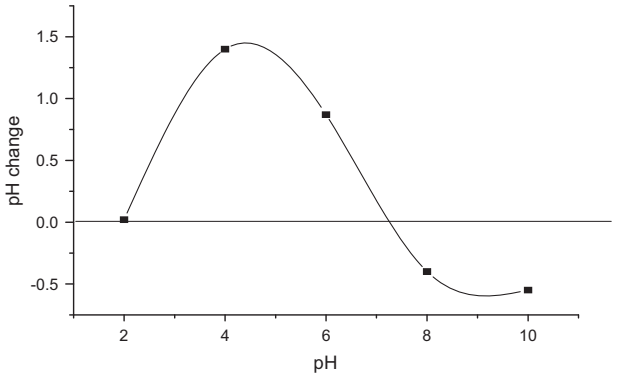

Figure 5 pH_{ZPC} of the experimental adsorbent.

F^- and negative charge of the AICFA. At pH 5, the surface of the AICFA is positive; hence, electrostatic attraction between positively charged AICFA surface and fluoride ions dose works well for fluoride removal. Almost similar type of interaction was reported by Junlian et al. [39]. They suggested that the adsorption of fluoride through the formation of inner-sphere surface complexes with the surface hydroxyl sites.

$$\equiv M{-}OH + H^+ + F^- \Longleftrightarrow \equiv MOH_2^+ \ldots\ldots F^- \quad (16)$$

$$\equiv M{-}OH + H^+ + F^- \Longleftrightarrow M^+ \ldots\ldots F^- + H_2O \quad (17)$$

$$\equiv M{-}OH + F^- \Longleftrightarrow M^+ \ldots\ldots F^- + OH^- \quad (18)$$

$$\equiv M{-}OH + Na^+ + OH^- + F^- \Longleftrightarrow M{-}O^- \ldots\ldots Na^+ \ldots..F^- + H_2O \quad (19)$$

3.3. Effect of adsorbate concentration

The effect of different concentration of fluoride solution on the adsorption process was studied under optimized conditions of shaking time and AICFA dose. Fig. 6 shows the proportional relationship between the fluoride concentration and the adsorbed amount of fluoride. However, increase in fluoride concentration above 3 mg/L, reduced fluoride removal (4%), probably due to saturation of adsorption sites on the surface.

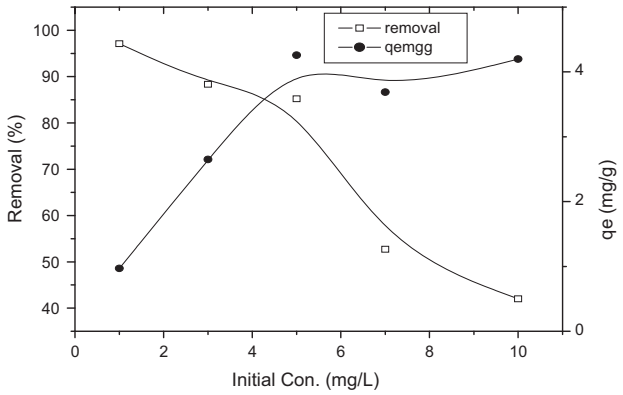

Figure 6 Effect of initial concentration (mg/L) on removal of fluoride from water (adsorbent dosage = 0.05 g/L, contact time = 1 h, pH = 6.5, temperature = 313 K).

Therefore, the present experiment suggests that AICFA can remove >88% F^- from water if its concentration is below 3 mg/L. The saturation behavior of adsorbent under such low level of fluoride is probably due to the fact that ratio of surface active sites to total fluoride is high; hence, the fluoride ions could interact with the adsorbent surface to occupy the active sites on the AICFA surface sufficiently, a significant factor that favors fluoride removal [40]. A similar study on fluoride adsorption was reported using $KMnO_4$-modified activated carbon derived from stem pyrolysis of rice straw [41].

3.4. Effect of AICFA

The removal efficiency of anions by any sorbent is closely related to its adsorption sites [42]. The defluoridation efficiency by AICFA dose is shown in Fig. 7a. Fig. 7a showed that when adsorbent amount increased from 0.2 to 1 g L^{-1}, the fluoride removal increased from 90.1% to 97.1%, respectively. This higher adsorption is probably due to larger surface available to sorption which promoted the sorption of fluoride [43]. On the other hand, Fig. 7b shows that the K_D increases with an increase in adsorbent dose at constant pH (5.0) that implies that the surface of AICFA is not completely homogeneous. If the surface is completely homogeneous, the K_D values at a given pH should not change with adsorbent dose.

3.5. Effect of contact time

Fig. 8 shows fluoride removal at different contact time using AICFA as an adsorbent. With increasing contact time, fluoride removal increased rather rapidly, but then dropped at 60 min and approached a more or less constant value denoting attainment of equilibrium. The sorption of fluoride is very rapid in less than 60 min. This may be the result of the instantaneous sorption reaction in which fluoride sorbed quickly on to the surface of AICFA. Moreover, the sudden rise in removal of fluoride (from 20 min to 40 min) indicates that the adsorption of fluoride probably takes place due to the diffusion taking place into the pores on the surface of the adsorbent [44]. After 60 min, fluoride removal rate leveled off significantly, denoting attainment of equilibrium and the nonavailability of sorption sites. The present results are in very good agreement with those of Nasr et al. [43]. As no further significant removal of fluoride

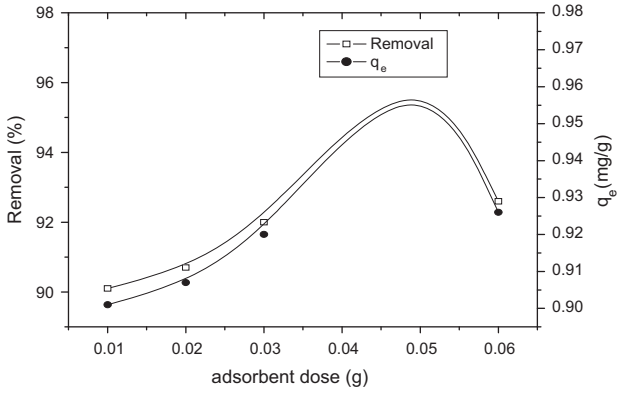

Figure 7a Effect of adsorbent dose (g) on removal of fluoride from water (initial conc. = 1 mg/L, pH = 5, contact time = 0.5 h, temperature = 313 K).

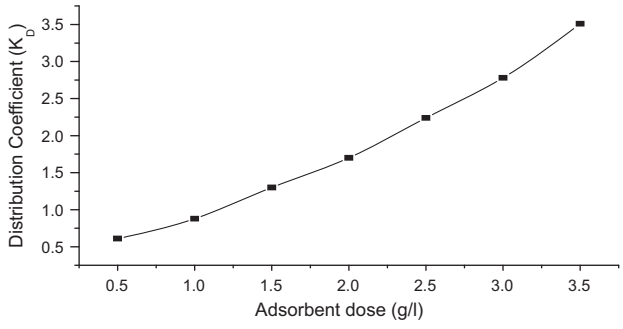

Figure 7b Plot of K_D value as a function of adsorbent dose (g/L) (pH 5.0). $[F^-]_{initial}$ dose 0.5–3.5 g/L, $pH_{initial} \approx 5.0$, volume of solution 0.1 L; contact time 60 min; shaking speed 450 rpm.

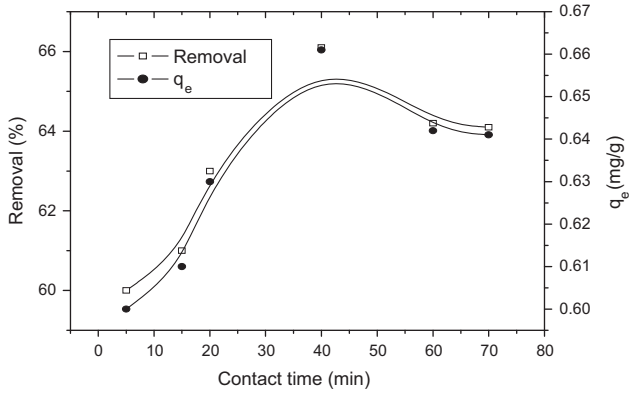

Figure 8 Effect of contact time (min) on removal of fluoride from water (initial conc. = 1 mg/L, adsorbent dosage = 0.05 g/L, pH = 5, temperature = 313 K).

was recorded after 60 min, an equilibrium time of 60 min was chosen and this was used in all subsequent experiments.

3.6. Effect of temperature

Fig. 9 shows that temperature exerts striking effect on the adsorption process. As temperature increased, the uptake of

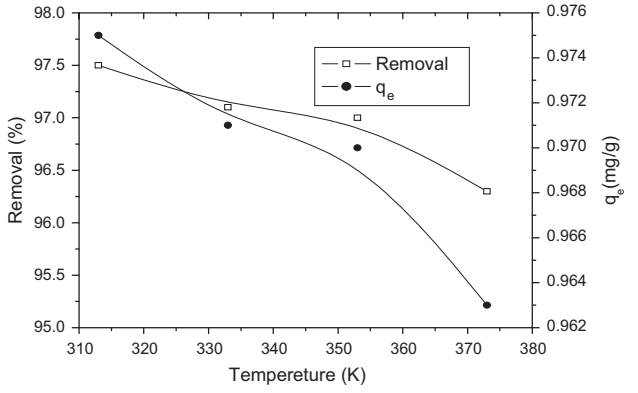

Figure 9 Effect of temperature (K) on removal of fluoride from water (initial conc. = 1 mg/L, adsorbent dosage = 0.05 g/L, pH = 5, contact time = 40 min.).

F^- onto AICFA decreased. Probably rise of temperature affects the solubility of F^- and it tends to escape from the solid phase to the bulk solution phase with increasing temperature. Sujana et al. [13] reported that the exothermic nature of adsorption of *F* on alum sludge existed because the rising temperature increased the tendency for *F* to escape from the adsorbent. Another reason given was an increase in thermal energy of adsorbed *F* at higher temperatures, causing increased desorption. Our results showed good agreement with many other earlier studies [41,44,45].

3.7. Effect of co-ions on fluoride removal

Previous reports have shown that some coexisting anions such as Cl^-, NO_3^-, SO_4^{2-}, HCO_3^-, CO_3^{2-}, and PO_4^{3-} could interfere in the fluoride adsorption process [46,47]. Present study evaluates the fluoride adsorption behavior in the presence of 100 mg L^{-1} salt solutions of nitrate, chloride, sulfate and phosphate independently, at the initial fluoride concentration of 1.0 mg L^{-1}. The interference of these co-ions on *F* removal is shown in Fig. 10. Fig. 10 reveals that fluoride removal is decreased from 93.08% to 81.34% in the presence of sulfate and to 66.22% in the presence of phosphates. However, slightly increased removal was noticed in the presence of chloride and nitrate ions. It is quite possible because some anions would enhance columbic forces and some would compete with fluoride for the active sites [48]. On the other hand, it is reported that, multivalent anions are adsorbed more readily than monovalent anions [49]. The relative performance of fluoride removal in the presence of anions increased in the order $PO_4^{3-} < SO_4^{2-} < Cl^- < NO_3^-$. This can be nicely explained with the help of *z*/*r* (charge/radius) values of the anions, which is in the order of PO_4^{3-} (3/3.40) > SO_4^{2-} (2/2.40) > Cl^- (1/1.81) > NO_3^- (1/2.81). Very similar results are also reported by Chen et al. [2] for removal of fluoride by granular ceramic [2].

3.8. Isotherm study

The isotherm constants were calculated from the slope and intercept of Langmuir, Freundlich and D–R isotherms and are presented in Table 1. The equilibrium parameter R_L, which is defined as $R_L = 1/(1 + bC_{A0})$, in the range of $0 < R_L < 1$

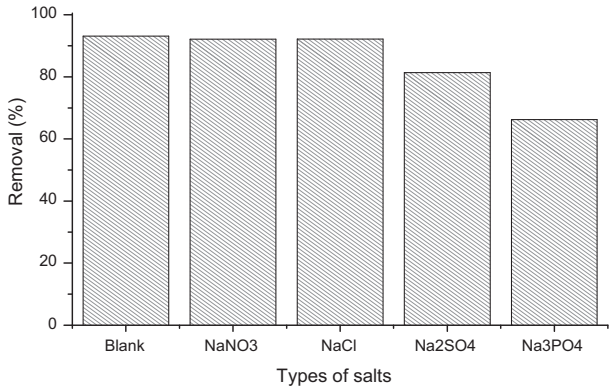

Figure 10 Effect of interfering ions for fluoride removal on AICFA (adsorbent dose 0.5 g L^{-1}, initial fluoride concentration 1 mg L^{-1}, equilibrium contact time 1.0 h, initial pH 5.0 and temperature 313 K).

reflects the favorable adsorption process [50]. In the present investigation the equilibrium parameter was found to be in the range of $0 < R_L < 1$ (results are not shown). This indicated the fact that the sorption process is very favorable and the adsorbent has a good potential for fluoride removal [40]. Again, Langmuir and Freundlich adsorption isotherm constants usually do not provide any idea about the mechanisms of adsorption [51]. In order to understand the adsorption type, whether physical or chemical, equilibrium data were tested with Dubinin–Radushkevich isotherm. The value of R^2 was higher for both D–R and Langmuir than Freundlich isotherm. Moreover, The values of D–R isotherm constants, β (mol^2/J^2) and q_m (mg/g) were calculated from the slope and intercept of the plot. The values of β are found as 0.581, 0.593, 0.611 and 0.732 $mol^2\ kJ^{-2}$ at 313, 333, 353 and 373 K, respectively. Similarly, the corresponding values of q_m are obtained as 3.412, 5.621, 5.718 and 5.331 mg/g. The value of β is found to be increasing along with increasing temperature while the value of q_m shows increasing trend from 313 to 353 K, but is decreased at 373 K. The mean adsorption energy (E) is usually employed to differentiate the process of adsorption between chemical and physical. If the value of E is in between 8 and 16 kJ/mol, the adsorption process is said to be chemical while the value below 8 kJ/mol indicates physical adsorption [52,53]. The values of E as determined using Eq. (9) for adsorption of fluoride on AICFA were found as 0.927, 0.918, 0.946 and 0.826 kJ/mol, respectively at the experimental temperatures indicated earlier. As all these values are less than 8 kJ/mol, the fluoride adsorption on AICFA seems to be physisorption in nature. Physical adsorption usually provides better regeneration scope [53].

Overall, using the linearized forms of different adsorption isotherm models, it is observed that for fluoride adsorption by AICFA, Langmuir isotherm fits well for other selected temperatures except at 313 K. Freundlich isotherm fits well only at 353 K.

3.9. Kinetic study

The kinetics of any sorption process is a function of different parameters, such as the structural properties of adsorbent, nature and concentration of adsorbate and adsorbent–adsorbate interactions [54,55]. Adsorption kinetic study was carried out with initial fluoride concentration of 1.0 mg L^- and adsorbent dose of 0.5 g L^{-1} at 313 K. Pseudo-first-order and pseudo-second-order adsorption model and intra-particle diffusion model were used to test the kinetic data in order to establish the mechanism of adsorption. The models are shown in Eqs. (10)–(12), respectively [56,57] and the output of kinetics constants are given in Table 2. The plot of intraparticle diffusion is shown in Fig. 11. The plot reflects three stage maturities, with an initial linear portion (a) followed by an intermediate linear portion (b) and a sharp linear portion (c). The initial curve of the plot is due to the diffusion of F^- through the solution to the external surface of AICFA or to the boundary layer. The second linear portion of curve describes the intra-particle diffusion of F^- on AICFA surface, and the last portion is the adsorption equilibrium stage [58,59]. Moreover, it is observed that the second portion did not pass through the origin, indicating that the adsorption mechanism on AICFA is probably complex and both the external adsorption and intra-particle diffusion contribute to the adsorption process [60]. This is further supported by calculating the intraparticle diffusion coefficient ($\overline{D}$) using Eq. (13). According to Michelson et al. [61] a $\overline{D}$ value of the order in $10^{-11}\ Cm^2\ S^{-2}$ is indicative of intraparticle diffusion as rate determining step. In this investigation, the value of $\overline{D}$ ($2.81 \times 10^{-8}\ Cm^2\ S^{-2}$) was obtained in the order of $10^{-8}\ Cm^2\ S^{-2}$ which is more than three orders of higher magnitude. It indicates that the intra-particle diffusion is not only the rate controlling step. It is concluded that both boundary layer and intraparticle diffusion may be involved in this F removal process.

3.10. Thermodynamic study

The values of ΔG°, ΔH° and ΔS° are shown in Table 3. The results show that ΔG° is negative, which indicates that adsorption of F^- on AICFA is a spontaneously process and the negative value of ΔH for the reaction indicates the exothermic nature of the reaction. Therefore, lower temperature promotes fluoride adsorption. The ΔS° is positive, which suggests increased randomness at the solid/solution interface during fluoride adsorption.

3.11. Fluoride removal from groundwater

In order to assess the potential application of AICFA for removal of fluoride from drinking water, tests were conducted

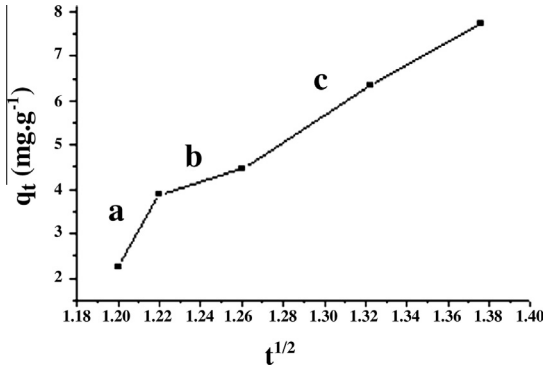

Figure 11 Intra-particle diffusion.

Table 3 Thermodynamic parameters for fluoride adsorption on AICFA.

ΔH° (kJ mol^{-1})	ΔS° (kJ mol^{-1})	ΔG° (kJ mol^{-1})			
		331 K	333 K	353 K	373 K
−34.90	116.29	−9.534	−9.720	−10.202	−10.177

with tube well water samples collected from the fluoride contaminated village of Nasipur, Birbhum district, West Bengal, India. Various water parameters of the groundwater samples were analyzed and are shown in Table 4. Defluoridation of samples of groundwater was conducted without adjusting pH of the experimental samples at the rate 0.5 g/L AICFA under identical experimental conditions of the equilibrium batch adsorption study. It was found that the fluoride levels in groundwater could come down to < 0.96 mg/L.

3.12. Regeneration

Water purification by adsorption technology is considered economical when the adsorbent is regenerable. Moreover, reuse of adsorbent helps to reduce environmental impacts of disposal of the used adsorbents. Desorption studies were carried out with 2 g/L fluoride adsorbed AICFA at varying pH by using 0.1 M NaOH. Fig. 12 shows that up to pH 8, there is no fluoride leaching. However, desorption of fluoride occurs better at pH greater than 8 and reaches maximum of 98% at pH 12. The adsorption capacity of regenerated AICFA reduces from 92% to 84% in first time and thereafter decreases gradually. It seems probably that at higher pH, OH— ions accumulated on fluoride loaded AICFA. Therefore, it is necessary to reactivate the AICFA under suitable pH medium for further use. Almost similar regeneration of adsorbent by varying concentration of NaOH solution was reported by Bhaumik and Mondal [42]. However, a further study is needed to assess the potentiality for reuse of AICFA.

3.13. Comparison with other adsorbents

The adsorption isotherms for the removal of fluoride ions from aqueous solution obtained in the present study were compared with those reported earlier in the literature (Table 5). However, direct comparison of AICFA with other adsorbents is difficult,

Table 4 Physico-chemical characteristics of groundwater samples.

Parameters	Nasipur
Conductivity (μS/cm)	102 ± 1.01
Hardness (mg/L, $CaCO_3$)	180 ± 2.66
Carbonate (mg/L)	ND
Chloride (mg/L)	10.1 ± 0.03
Nitrate (mg/L)	8.7 ± 0.61
Sulfate (mg/L)	0.88 ± 1.02
Fluoride (mg/L)	6.01 ± 0.11
Sodium (mg/L)	106 ± 1.07
Calcium (mg/L)	12.5 ± 1.28
pH	7.80

Mean ± SD.

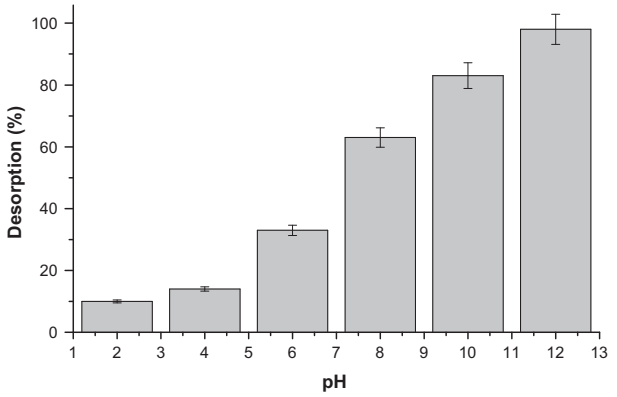

Figure 12 Regeneration of adsorbent (AICFA) at different pH.

Table 5 Comparison of the defluoridation capacities of different biomass carbon and modified biomass causes.

Adsorbent	pH	Adsorption capacity (mg g^{-1})	References
Eichhormia crassipes Biomass Carbon at 300 °C	5.8	0.52	[62]
Biomass Carbon at 600 °C		1.54	[62]
Moringa indica based activated carbon	2.0	0.23	[63]
Used tea waste carbon			[18]
Activated carbon derived from rice strand	2.0	15.90	[41]
Pine wood biochar	2.0	7.66	[21]
Pine wood biochar	2.0	9.77	[21]
Ammonium carbonate activated carbon of Tamarindus indica fruit shell	7.05	22.33	[3]
Zirconium(iv)-impregnated groundnut (Anacardium occidentale) shell carbon		2.23	[64]
Cynodon dactylon-based activated carbon	7.0	4.617	[65]
Zirconium impregnated cashew nut (Anacardium occidental) shell carbon	7.0	1.83	[66]
Sugarcane bagasse carbon			[16]
Phyllanthus embolic based thermally activated carbon	7.0	7.014	[67]
Pecan (carya illinoinensis)nut shell carbon modified with egg shells calcium	7.0	1.61–2.51	[68]
Scandinavia spruce wood modified with aluminum and iron oxides carbonized at 500 °C	6.9	7.92	[69]
Scandinavia spruce wood modified with aluminum and iron oxides carbonized at 650 °C	6.9	5.67	[69]
Scandinavia spruce wood modified with aluminum and iron oxides carbonized at 900 °C	6.9	5.67	[69]
Activated bagasse carbon	6.0	1.15	[15]
Aluminum impregnated coconut fiber ash	5.0[a]	3.192[a]	Current studied

[a] Freundlich adsorption capacity.

and it was found, in general, that the adsorption capacity of AICFA for fluoride ions is comparable with that of other adsorbents and in fact greater than certain adsorbents reported earlier.

4. Conclusions

It is evident that the presence of fluoride in water supplies in many countries around the world is still a problem to be solved. Application of aluminum loaded adsorbent, which is one of the modified forms of coconut fiber, has been reported in the present paper for fluoride removal from aqueous solutions and some of the important conclusions have been drawn. Aluminum impregnated coconut fiber ash (AICFA) has significant potential in the removal of fluoride from fluoride contaminated water even in the presence of nitrates and others anions (bicarbonate, sulfate, etc.). XRD and SEM study reveals that impregnation with Al on coconut fiber is quite well and uniform. The presence of chemical functional groups such as hydroxyl, carbonyl, and amine on the biosorbent surface contributes to biosorption. pH of the media has significant effect on F^- removal and is best at pH 5. Quantitative fluoride removal from water confirms the validity of these obtained results and the adsorption data for fluoride onto AICFA were better correlated to the Langmuir than to the Freundlich isotherm. In the adsorption kinetic modeling studies, the pseudo-second order chemical reaction kinetics provided the best correlation of the experimental data for AICFA. These kinetic data would be useful for developing an appropriate technology in designing a treatment plant for fluoride rich water. The maximum static adsorption capacity is recorded as 3.192 mg g^{-1} at 313 K. Presence of polyvalent negative ions (PO_4^{3-} and SO_4^{2-}) has negative effect on fluoride adsorption. The regenerated AICFA shows lower fluoride adsorption performance than that of fresh one. The optimization of regeneration processes needs further investigation. Moreover, a best adsorbent along with suitable module for the removal of fluoride from groundwater may be developed from these results. This part has been left for future considerations.

Acknowledgments

This work was financially supported by the University of Burdwan, Burdwan, to the Department of Environmental Science. Moreover, authors extend their sincere thanks to Dr. Partha Mitra, Associate Professor, Department of Physics, The University of Burdwan for his kind cooperation and necessary instrumental help.

References

[1] V. Tomar, D. Kumar, A critical study on efficiency of different materials for fluoride removal from aqueous media, Chem. Central J. 7 (2013) 2–15.
[2] N. Chen, Z. Zhang, C. Feng, N. Sugiure, M. Li, R. Chen, Fluoride removal from water by granular ceramic adsorption, J. Colloid Interf. Sci. 348 (2010) 579–584.
[3] V. Sivasankar, S. Murugesh, S. Rajkumar, A. Darchen, Cerium dispersed in carbon (C_eDc) and its adsorption behavior: a first example of tailored adsorbent for fluoride removal from drinking water, Chem. Eng. J. 2013 (2014) 45–54.
[4] S. Ayoob, A.K. Gupta, Fluoride in drinking water: a review on the status and stress effects, Crit. Rev. Environ. Sci. Technol. 36 (2006) 433–487.
[5] D.L. Ozsvath, Fluoride and environment health: a review, Rev. Environ. Sci. Biotechnol. 8 (2009) 59–79.
[6] M.H. Trivedi, R.J. Verma, N.J. Chinmay, R.S. Patel, N.G. Sathawara, Effect of high fluoride water on intelligence of school children in India, Fluoride 40 (2007) 178–183.
[7] E. Adamek, K. Pawlowska-Goral, K. Bober, In nitro and in Nino effects of fluoride ions on enzyme activity, Ann. Acad., Med. Stein. 51 (2005) 69–85.
[8] WHO (World Health Organization), Guidelines for Drinking Water Quality, World Health Organization, Geneva, 2004.
[9] WHO (World Health Organization), Guidelines for Drinking Water Quality, World Health Organization, Geneva, 1993.
[10] P.I. Ndiaye, P. Moulin, L. Dominguez, J.C. Millet, F. Charbit, Removal of fluoride from electronic industrial effluent by RO membrane separation, Desalination 173 (2005) 25–32.
[11] E. Antwi, E.C. Bensah, J.C. Ahiekpor, Use of solar water distiller for treatment of fluoride-contaminated water: the case of Bongo district of Ghana, Desalination 278 (2011) 333–336.
[12] M.W. Fang, L.W. Jun, C.G. Wei, Factors influencing the removal of fluoride from groundwater by nanofiltration, in: Proceeding of 3rd International Conference on Bioinformatics and Biomedical Engineering, Beijing. China, 2009.
[13] M.G. Sujana, R.S. Thakur, S.B. Rao, Removal of fluoride from aqueous solution by using alum sludge, J. Colloid Interf. Sci. 206 (1998) 94–101.
[14] C.J. Haung, J.C. Liu, Precipitate flotation of fluoride-containing wastewater from a semiconductor manufacturer, Water Res. 33 (1999) 3403–3412.
[15] S. Bibi, A. Farooqi, K. Hussain, N. Haider, Evaluation of industrial based adsorbents for simultaneous removal of arsenic and fluoride from drinking water, J. Cleaner Product. 87 (2015) 882–896.
[16] N.K. Mondal, R. Bhaumik, P. Roy, B. Das, J.K. Datta, Investigation on fixed bed column performance of fluoride adsorption by sugarcane charcoal, J. Environ. Biol. 34 (2013) 1059–1064.
[17] E. Kumar, A. Bhatnagar, M. Ji, W. Jung, S.H. Lee, S.J. Kim, G. Lee, H. Song, J.Y. Choi, J.S. Yang, B.H. Jeon, Defluoridation from aqueous solutions by granular ferric hydroxide (GFH), Water Res. 43 (2009) 490–498.
[18] N.K. Mondal, B. Das, R. Bhaumik, P. Roy, Calcareous soil as a promising adsorbent to remove fluoride from aqueous solution: equilibrium, kinetic and thermodynamic study, J. Modern Chem. Chem Technol. (2012) 1–21.
[19] N.K. Mondal, R. Bhaaumik, T. Baur, B.A. Das, P. Roy, J.K. Datta, Studies on defluoridation of water by tea ash: an unconventional biosorbent, Chem. Sci. Trans. 1 (2012) 239–256.
[20] R. Bhaumik, N.K. Mondal, B. Das, P. Roy, K.C. Pal, C. Das, A. Banerjee, J.K. Datta, Egg shell powder as an adsorbent for removal of fluoride from aqueous solution: equilibrium, kinetics and thermodynamics study, E-J. Chem. 9 (3) (2012) 1457–1480.
[21] S.V. Mohan, S.V. Ramanaiah, B. Rajkumar, P.N. Sarma, Biosorption of fluoride from aqueous phase onto algal Spirogyra sp IO1 and evaluation of adsorption kinetics, Bioresource Technol. 98 (2007) 1006–1011.
[22] S. Deng, H. Liu, W. Zhou, J. Huang, G. Yu, Mn–Ce oxide as a high-capacity adsorbent for fluoride removal from water, J. Hazard. Mater. 186 (2011) 1360–1366.
[23] S. Hunt, Diversity of biopolymer structure and its potential for ion-binding applications, in: H. Eccles, S. Hunt (Eds.), Immobilization of Ions by Biosorption, Ellis Horwood Limited, Chichester, England, 1986, pp. 15–46.
[24] B. Greene, R. McPherson, D. Damall, Algal sorbents for selective metal ion recovery, in: J.W. Patterson, R. Pasino

(Eds.), Metals Speciation, Separation and Recovery, Lewis, Chelsea, MI, 1987, pp. 315–338.
[25] H. Mann, Biosorption of heavy metals by bacterial biomass, in: B. Molesky (Ed.), Biosorption of Heavy Metals, CRC Press, Boca Raton, FL, 1990, pp. 93–137.
[26] V. Ganvir, K. Das, Removal of fluoride from drinking water using aluminum hydroxide coated rice husk ash, J. Hazard. Mater. 185 (2011) 1287–1294, http://dx.doi.org/10.1016/j.jhazmat.2010.10.044.
[27] WHO, Chemical Fact Sheets: Fluoride, Guidelines for Drinking Water Quality (Electronic Resource), in: Incorporation First Addendum, Recommendations, vol. 1, third ed., Geneva, 2006, pp. 375–377.
[28] A. Tor, N. Danaoglua, G. Arslan, Y. Cengeloglu, Removal of fluoride from water by using granular red mud: batch and column studies, J. Hazard. Mater. 164 (2009) 271–278.
[29] S.S. Tripathy, A.M. Raichur, Abatement of fluoride from water using manganese dioxide-coated activated alumina, J. Hazard. Mater. 153 (2008) 1043–1051.
[30] S.K. Swain, T. Padhi, T. Patnaik, R.K. Patel, U. Jha, R.K. Dey, Kinetics and thermodynamics of fluoride removal using cerium-impregnated chitosan, Desalination Water Treat. 13 (2010) 369–381.
[31] L. Sigg, Chemical processes at the particle water-interface, in: S. Werner (Ed.), Aquatic Surface Chemistry, John Wiley & Sons, New York, 1987, p. 325.
[32] P. Zhou, X. Zhu, J. Yu, W. Xiao, Effects of adsorbed F, OH, and Cl ions on formaldehyde adsorption performance and mechanism of anatase TiO_2 nanosheets with exposed 001 facets, Appl. Mater. Interf. 5 (2012) 8165–8172.
[33] R.S. Sathish, S. Sairam, V.G. Raja, G.N. Rao, C. Janardhana, Defluoridation of water using Zirconium impregnated coconut fiber carbon, Separ. Purif. Technol. 43 (2008) 3676–3694.
[34] T.S. Singh, K.K. Pant, Equilibrium, kinetics and thermodynamic studies for adsorption of As(III) on activated alumina, Separ. Purif. Technol. 36 (2004) 139–147.
[35] E. Vences-Alvarez, L.H. Velazquez-Jimenez, L.F. Chazaro-Ruiz, P.E. Diaz-Flores, J.R. Rangel-Mendez, Fluoride removal in water by a hybrid adsorbent lanthanum–carbon, J. Colloid Interface Sci. 455 (2015) 194–202.
[36] M. Mourabet, A. El Rhilassi, H. El Boujaady, M. Bennani-Ziatni, A. Taitai, Use of response surface methodology for optimization of fluoride adsorption in an aqueous solution by Brushite, Arabian J. Chem. (2014), http://dx.doi.org/10.1016/j.arabjc.2013.12.028.
[37] N. Calace, E. Nardi, B.M. Petronio, M. Pietroletti, Adsorption of phenols by paper-mill sludges, Environ. Pollut. 118 (2002) 315–319.
[38] M.K. Mondal, Removal of Pb(II) ions from aqueous solution using activated tea waste: adsorption on a fixed-bed column, J. Environ. Manage. 90 (2010) 3266–3271.
[39] Q.I.A.O. Junlian, C.U.I. Zimin, S.U.N. Yuankui, H.U. Qinghai, Q.U.A.N. Xiaohong, Simultaneous removal of arsenate and fluoride from water by Al–Fe (hydr)oxides, Frontiers Environ. Sci. Eng. 8 (2) (2014) 169–179.
[40] S.F. Montanher, E.A. Oliveira, M.C. Rollemberg, Removal of metal ions from aqueous solutions by sorption onto rice bran, J. Hazard. Mater. B117 (2005) 207–211.
[41] A.A.M. Daifullah, S.M. Yakout, S.A. Elreefy, Adsorption of fluoride n aqueous solutions using $KMnO_4$-modified activated carbon derived from steam pyrolysis of rice straw, J. Hazard. Mater. 147 (2007) 633–643.
[42] R. Bhaumik, N.K. Mondal, Optimizing adsorption of fluoride from water by modified banana peel dust using response surface modelling approach, Appl. Water Sci. (2014), http://dx.doi.org/10.1007/s13201-014-0211-9.
[43] A.B. Nasr, K. Walha, C. Charcosset, R.B. Amar, Removal of fluoride ions using cuttlefish bones, J. Fluorine Chem. 132 (2011) 57–62.
[44] D. Das, J. Das, K. Parida, Physicochemical characterization and adsorption behaviour of calcined Zn/Al hydrotalcite-like compound (HT/c) towards removal of fluoride from water, J. Colloid Interf. Sci. 261 (2003) 213–220.
[45] D. Mahapatra, D. Mishra, S.P. Mishra, G.R. Choudhury, R.P. Das, Use of oxide minerals to absorbed fluoride from water, J. Colloid Interf. 275 (2004) 355–359.
[46] R.R. Devi, I.M. Umlong, P.K. Raul, B. Das, S. Banerjee, L. Singh, Defluoridation of water using nano-magnesium oxide, J. Exp. Nanosci. 9 (2014) 512–524.
[47] L.-X. Li, D. Xu, X.-Q. Li, W.-C. Liu, Y. Jia, Excellent fluoride removal properties of porous hollow MgO microspheres, New J. Chem. 38 (2014) 5445–5452.
[48] M.S. Onyango, Y. Kojima, O. Aoyi, E.C. Bernardo, H. Matsuda, Adsorption equilibrium modeling and solution chemistry dependence of fluoride removal from water by trivalent-cation-exchanged zeolite F-9, J. Colloid Interf. Sci 279 (2004) (2004) 341–350.
[49] L. Lv, J. He, M. Wei, D.G. Evans, Z. Zhou, Treatment of high fluoride concentration water by MgAl–CO_3 layered double hydroxides: kinetic and equilibrium studies, Water Res. 41 (2007) 1534–1542.
[50] A.K. Bhattacharya, S.N. Mandal, S.K. Das, Adsorption of Zn (II) from aqueous solution by using different adsorbents, Chem. Eng. J. 123 (2006) 43–51.
[51] M. Islam, P.C. Mishra, R.K. Patel, Physicochemical characterization of hydroxy-apatite and its application towards removal of nitrate from water, J. Environ. Manage. 91 (2010) 1883–1891.
[52] S.K. Swain, S. Mishra, T. Patnaik, R.K. Patel, R.K. Dey, U. Jha, Fluoride removal performance of a new hybrid sorbent of Zr(IV)–ethylenediamine, Chem. Eng. J. 184 (2012) 72–81.
[53] S.N. Milmile, J.V. Pande, S. Karmakar, A. Bansiwal, T. Chakrabarti, R.B. Biniwale, Equilibrium isotherm and kinetic modeling of the adsorption of nitrates byanion exchange Indion NSSR resin, Desalination 276 (2011) 38–44.
[54] P. Mondal, S. George, A review on adsorbents used for defluoridation of drinking water, Rev. Environ. Sci. Biotechnol. (2015), http://dx.doi.org/10.1007/s11157-014-9356-0.
[55] S. Sadaf, H.N. Bhatti, Evaluation of peanut husk as a novel, low cost biosorbentfor the removal of Indosol Orange RSN dye from aqueous solutions: batch and fixed bed studies, Clean Technol. Environ. Policy 16 (2014) 527–544, http://dx.doi.org/10.1007/s10098-013-0653-z.
[56] I.B. Solangi, S. Memon, M.I. Bhanger, An excellent fluoride sorption behaviour of modified amberlite resin, J. Hazard. Mater. 176 (2010) 186–192.
[57] W.J. Weber Jr., J.C. Morris, Kinetics of adsorption on carbon from Solution, J. Sanit. Eng. Div. An. Sot. Civ. Eng. 89 (1963) 31–60.
[58] V.K. Gupta, I. Ali, V.K. Saini, Defluoridation of wastewater using waste carbon slurry, Water Res. 41 (2007) 3307–3316.
[59] S.P. Kamble, G. Deshpande, P.P. Brave, S. Rayalu, N.K. Labhsetwar, A. Malyshew, B.D. Kulkarni, Adsorption of fluoride from aqueous solution by alumina of alkoxide nature: batch and continuous operation, Desalination 264 (2010) 15–23.
[60] Y.S. Ho, Review of second-order models for adsorption systems, J. Hazard. Mater. 136 (2006) 681–689.
[61] L.D. Michelson, P.G. Gideon, E.G. Pace, L. Kutsal, US Dept. Industry, office of the water research and technology, Bulletin (1975) 74.
[62] S. Sinha, K.P. Pandey, D. Mohan, K.P. Singh, Removal of fluoride from aqueous solutions by Eichhornia crassipes

biomass and its carbonizsed form, Ind. Eng. Chem. Res. 42 (2003) 6911–6918.
[63] G. Karthikeyan, S.S. Llango, Fluoride sorption using Moringa indica based activated carbon, Iranian J. Environ. Health Sci. Eng. 4 (2007) 21–28.
[64] G. Alagumuthu, M. Rajan, Equilibrium and kinetics of adsorption of fluoride onto zirconium impregnated cashew nut shell carbon, Chem. Eng. J. 158 (2010) 451–457.
[65] G. Alagumuthu, V. Veeraputhiran, R. Venkataraman, Fluoride sorption using Cynodon dactylon-based activated carbon, Hem. Ind. 65 (2011) 23–35.
[66] G. Alagumuthu, M. Rajan, Kinetic and equilibrium studies on fluoride removal by zirconium (IV) impregnated groundnut shell carbon, Hem. Ind. 64 (2010) 295–304.
[67] V. Veeraputhiran, G. Alagumuthu, Sorption equilibrium of fluoride onto Phyllanthus emblica activated carbon, Inter. J. Res. Chem. 1 (2011) 42–47.
[68] V. Hernández-Montoya, L.A. Ramírez-Montoya, A. Bonilla-Petriciolet, M.A. Montes-Morán, Optimizing the removal of fluoride from water using new carbons obtained by modification of nut shell with a calcium solution from egg shell, Biochem. Eng. J. 62 (2012) 1–7.
[69] E. Tchomgui-Kamga, V. Alonzo, C.P. Nanseu-Njiki, N. Audebrand, E. Ngameni, A. Darchen, Preparation and characterization of charcoals that contain dispersed aluminum oxide as adsorbents for removal of fluoride from drinking water, Carbon 48 (2010) 333–343.